ELSEVIER

Available online at www.sciencedirect.com

SCIENCE DIRECT®

Journal of Solid State Chemistry 178 (2005) 2635–2642

JOURNAL OF SOLID STATE CHEMISTRY

www.elsevier.com/locate/jssc

Synthesis and characterization of homo- and heterobimetallic niobium^{V} and tantalum^{V} peroxo-polyaminocarboxylato complexes and their use as single or multiple molecular precursors for Nb–Ta mixed oxides

Daisy Bayot, Matthieu Degand, Michel Devillers*

Université Catholique de Louvain. Unité de Chimie des Matériaux Inorganiques et Organiques, place Louis Pasteur 1/3,
B-1348 Louvain-la-Neuve, Belgium

Received 16 March 2005; received in revised form 31 May 2005; accepted 1 June 2005

Abstract

New water-soluble bimetallic peroxo complexes of niobium^{V} and/or tantalum^{V} with high-denticity polyaminocarboxylate ligands have been prepared, characterized from the spectroscopic point of view, and used as molecular precursors for Nb–Ta mixed oxides. Four new homobimetallic complexes, $(gu)_3[Nb_2(O_2)_4(dtpaO_3)]\cdot 3H_2O$ **1**, $(gu)_3[Ta_2(O_2)_4(dtpaO_3)]\cdot 5H_2O$ **2**, $(gu)_3[Nb_2(O_2)_4(HtthaO_4)]\cdot 2H_2O$ **4** and $(gu)_3[Ta_2(O_2)_4(HtthaO_4)]\cdot 3H_2O$ **5** and the corresponding heterometallic complexes, $(gu)_3[NbTa(O_2)_4(dtpaO_3)]\cdot 2.5H_2O$ **3** and $(gu)_3[NbTa(O_2)_4(HtthaO_4)]\cdot 2H_2O$ **6** have been obtained. In these compounds, the in situ oxidation of the nitrogen atoms of the PAC ligands into N-oxide groups has been evidenced by IR spectroscopy and mass spectrometry. The thermal treatment of the homonuclear complexes in air at 700 or 800 °C, depending on the Ta content, provided Nb_2O_5 or Ta_2O_5 while the heteronuclear compounds led to the solid solution $TaNbO_5$. BET and SEM measurements have been carried out and comparison of the morphology of the samples prepared from homo- and heterometallic precursors is discussed.

Keywords: Niobium; Tantalum; Polyaminocarboxylate; Peroxo complexes; Precursors; Mixed oxides

1. Introduction

In recent years, multimetallic Nb-containing oxides have generated considerable interest in many fields, because of their attractive physical properties: for example, such oxides are widely studied as ferroelectric and piezoelectric materials like $BiNbO_4$ [1], as ion conductors like Y_3NbO_7 [2], and also as promising catalysts in several highly challenging processes, like water photodecomposition [3–8], alkane oxidation or ammoxidation [9,10]. Within the same context, analogous Ta-based oxides, like $BiTaO_4$ [6,11] and $TaVO_5$ [12], were also reported but in a very less extended way than for niobium. The literature describes mainly solid solutions between niobium and tantalum pentoxides, of general formula $(Ta_xNb_{1-x})_2O_5$ [13–15]. Such materials are mainly studied as photocatalysts for water decomposition [3–5].

The conventional way to prepare oxide materials is based on solid-state reactions between the binary oxides. This so-called "ceramic method" requires heat treatments at a relatively high temperature, as well as repeated grinding procedures, and generally results in oxides of low purity. Because of these limitations, alternative routes such as sol-gel synthesis, citrate method, metal-organic chemical vapor deposition (MOCVD) or pyrolytic decomposition are often considered. These methods, requiring metal-organic precursors which have specific chemical and physical

---

*Corresponding author. Fax: + 32 10 472330.
E-mail address: devillers@chim.ucl.ac.be (M. Devillers).

0022-4596/$ - see front matter © 2005 Elsevier Inc. All rights reserved.
doi:10.1016/j.jssc.2005.06.001

properties, present some obvious advantages: (i) the use of molecular precursors provides homogeneous materials; (ii) these "precursor routes" allow to form crystalline oxides under conditions significantly milder than those employed in conventional solid-state synthesis [16,17] and result in materials with relatively high specific surface areas and (iii) the presence of bridging or chelating organic ligands in the precursors has been shown to avoid unwanted metal segregation during oxide formation [18]. More particularly, when different metals are involved in the final oxide formulation, the main advantage of such routes is the potential use of heterometallic single-source precursors, when available. A single-source precursor provides a direct route to advanced materials and may lead to a higher quality of products because of a much greater control of the metal stoichiometry in the final oxide [19–21]. Ideally, heteronuclear precursor complexes containing the number of metal atoms corresponding to the stoichiometry of the desired oxide phase are required to optimize the approach but this often represents an ambitious challenge.

The Nb- or Ta-based heterometallic compounds described so far are practically exclusively alkoxide-type precursors which, unfortunately, present several disadvantages such as their moisture sensitivity or expensiveness. The described heterometallic complexes of Nb or Ta with oxo and/or alkoxo ligands only are numerous. Compounds such as $Nb_2(OMe)_2(ReO_4)_2$, $M_2O_2(OMe)_{14}(ReO_4)_2$ (M = Nb or Ta) [22], $Mg[Nb(OEt)_6]_2 \cdot 2EtOH$, $Sr[Ta(OiPr)_6]_2 \cdot 2Pr^iOH$ [23], $Mo_4M_2O_8(O^iPr)_{14}$ and $Mo_4M_4O_{16}(O^iPr)_{12}$ (M = Nb or Ta) [24] have been reported recently. Next to that, it has been shown that the association of the metal alkoxides with ligands such as halides, acetate, carboxylates or β-diketonates can be considered as a way to overcome the difficulty of handling them. Several acetato-alkoxo-based heterometallic compounds with Nb such as $MNb_2(OAc)(O^iPr)_{10}$ (M = Mg, Cd or Pb) [18,25] have been studied as precursors for the corresponding MNb_2O_6 phase. Also, some acetylacetonate derivatives such as $M^{II}_2M^{V}_2(acac)_2(OMe)_{12}$ (M^{II} = Co, Ni, Zn or Mg and M^V = Nb or Ta) [26] are known. Moreover, very recently, two heterometallic Nb or Ta and Bi-based compounds with salicylate ligands, $Bi_2M_2(\mu\text{-}O)(sal)_4(Hsal)_4(OEt)_2$ and $BiM_4(\mu\text{-}O)_4(sal)(Hsal)_3(O^iPr)_4$ [20,21], have been reported as single-source precursors for the ferroelectric $BiMO_4$ phase. However, only two mixed niobium and tantalum heterometallic alkoxide-type complexes have been described so far: the homoleptic $NbTa(OMe)_{10}$ compound [27] and the heteroleptic $[Ta(O^iPr)_4]Nb(tea)$ compound (tea = triethanolamine) [28].

We reported very recently the synthesis and characterization of a mixed Nb–Ta peroxo-tartrato complex of stoichiometry $(gu)_5[NbTa(O_2)_4(tart)(Htart)] \cdot 4H_2O$, in which the tartrate is a tetradentate and bridging ligand. This compound displays the advantages to be air-stable and water-soluble and it was engaged as a single-source precursor for the $TaNbO_5$ phase [29].

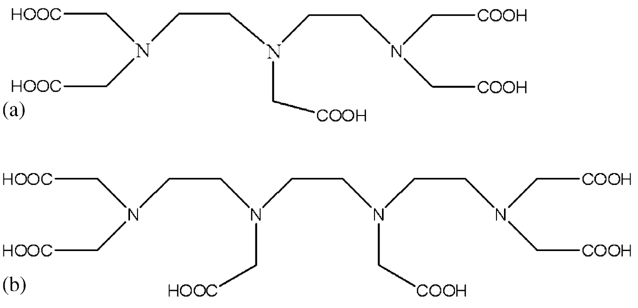

Scheme 1. Structures of the (a) H_5dtpa and (b) H_6ttha ligands.

In addition, we also studied water-soluble peroxo Nb^V or Ta^V mononuclear complexes with polyaminocarboxylato ligands like ethylenediaminetetraacetic (edta) and propylenediaminetetraacetic (pdta) acids, for which the synthesis in the presence of excess H_2O_2 was shown to lead to an in situ oxidation of both nitrogen atoms of the PAC ligand into N-oxide groups [30,31].

We report here the synthesis and characterization of novel air-stable and water-soluble homo- and heterobimetallic peroxo complexes of Nb^V and Ta^V with polyaminocarboxylato ligands which display a higher denticity than edta and pdta, such as diethylenetriaminepentaacetic (dtpa) and triethylenetetraaminehexaacetic (ttha) acids. The structures of both ligands are illustrated in Scheme 1. They possess a high number of coordination sites, eight and ten, respectively, and therefore could lead to the formation of polynuclear complexes. We expected the in situ N-oxidation of the ligand as previously observed in the case of the edta and pdta species [30,31]. Next to that, the formation of a solid solution between Nb_2O_5 and Ta_2O_5 from the thermal decomposition of the prepared complexes is also investigated.

2. Experimental

2.1. General procedures

The peroxo-polyaminocarboxylato Nb^V and/or Ta^V complexes were prepared by substituting peroxo groups by a polyaminocarboxylate (PAC) ligand in the tetraperoxometallate anion(s), $[M(O_2)_4]^{3-}$. These syntheses were processed in the presence of excess hydrogen peroxide and led, as expected, to the direct formation of the N-oxide derivative of the PAC ligand. This in situ N-oxidation phenomenon was actually previously observed in the case of the edta or pdta peroxo complexes of niobium or tantalum [30,31]. Moreover, the (N-oxide)PAC ligands, H_5dtpaO_3 and H_6tthaO_4, were synthesized separately following procedures adapted from the work of Bertran-Porter et al. [32].

Diethylenetriaminepentaacetic acid, H_5dtpa (Fluka, >99%), triethylenetetraaminehexaacetic acid, H_6ttha (Sigma-Aldrich, 98%) and hydrogen peroxide, H_2O_2 (Acros, 35 wt%) were commercial products used as received. Elemental analyses (C, H, N) of the complexes were carried out at the University College of London. IR spectra in the 4000–400 cm^{-1} range were recorded on a FTS-135 Bio-RAD spectrometer, using KBr pellets containing ca 1 wt% of the powder. Thermogravimetric analyses (TGA) were performed in air at the heating rate of 10 °C min^{-1} using a Mettler Toledo TGA/SDTA851^e analyser. Nano-electrospray ionization mass spectrometry (NESI-MS) measurements were obtained on a Finnigan MAT LCQ instrument (San Jose, CA). The samples were introduced by injection of a 0.001 mol L^{-1} solution of the complex dissolved in CH_3OH/H_2O (1:1 vol.). Powder X-ray diffraction (XRD) was carried out on a SIEMENS D-5000 diffractometer using the Cu-Kα radiation ($\lambda = 1.5418$ Å). FT-Raman spectra were recorded on a Bruker spectrometer (type RFS100/S) at the wavelength of 1064 nm. BET specific surface areas were measured with a Micromeritics ASAP 2000 analyser using nitrogen at 77 K. The SEM studies were carried out on a DSM982 GEMINI microscope operating at a 1 kV accelerating voltage.

2.2. *Syntheses of the precursors*

All the manipulations were carried out in aqueous solution. The starting reactants, $(gu)_3[M(O_2)_4]$ (M = Nb or Ta) were previously synthesized, according to reported procedures [31,33], from niobic or tantalic acid in the presence of an excess of H_2O_2 and guanidinium carbonate, $(gu)_2CO_3$ (Aldrich). Niobic acid, $Nb_2O_5 \cdot nH_2O$ was supplied from CBMM (Brazil) and tantalic acid was prepared by hydrolysis of tantalum chloride, $TaCl_5$ (Alfa Aesar) in ammonia medium.

$(gu)_3[Nb_2(O_2)_4(dtpaO_3)] \cdot 3H_2O$ 1. $(gu)_3[Nb(O_2)_4]$ (1 g, 2.5 mmol) was dissolved in 20 mL distilled water and 5 mL of a 35 wt% H_2O_2 solution. H_5dtpa (0.491 g, 1.25 mmol) was added while stirring and pH was adjusted down to 3 with nitric acid (1 mol L^{-1}). The resulting clear solution was then gently heated for a few minutes ($T = 70$ °C). The subsequent addition of ethanol (150 mL) provided a white and fine solid. The suspension was stored at 5 °C during 24 h and the precipitate was finally filtered off, washed with ethanol and air-dried (0.91 g, 70%). Found: C, 21.09; H, 4.25; N, 16.71. $C_{17}H_{42}N_{12}Nb_2O_{24}$ requires C, 20.73; H, 4.27; N, 17.07%.

$(gu)_3[Ta_2(O_2)_4(dtpaO_3)] \cdot 5H_2O$ 2. $(gu)_3[Ta(O_2)_4]$ (0.752 g, 1.53 mmol) was dissolved in 20 mL distilled water and 5 mL of a 35 wt% H_2O_2 solution. H_5dtpa (0.302 g, 0.761 mmol) was added while stirring and pH was adjusted down to 3 with nitric acid (1 mol L^{-1}). The resulting clear solution was then gently heated for a few minutes ($T = 60$ °C). The subsequent addition of ethanol (150 mL) and storage at 5 °C during a few hours yielded a white precipitate which was filtered off, washed with ethanol and air-dried (0.40 g, 45%). Found: C, 16.70; H, 3.29; N, 11.79. $C_{13}H_{47}N_{15}Ta_2O_{26}$ requires C, 17.06; H, 3.85; N, 14.05%.

$(gu)_3[NbTa(O_2)_4(dtpaO_3)] \cdot 2.5H_2O$ 3. $(gu)_3[Nb(O_2)_4]$ (0.41 g, 1.02 mmol) and $(gu)_3[Ta(O_2)_4]$ (0.50 g, 1.02 mmol) were dissolved in 20 mL distilled water and 5 mL of a 35 wt% H_2O_2 solution. H_5dtpa (0.40 g, 1.02 mmol) was added while stirring and pH was adjusted down to 3 with nitric acid (1 mol L^{-1}). The resulting clear solution was then gently heated for a few minutes ($T = 60$ °C). The subsequent addition of ethanol (150 mL) and storage at 5 °C during a few hours yielded a white precipitate which was filtered off, washed with ethanol and air-dried (0.60 g, 55%). Found: C, 18.94; H, 3.58; N, 14.95. $C_{17}H_{41}N_{12}NbTaO_{23.5}$ requires C, 19.22; H, 3.86; N, 15.83%.

$(gu)_3[Nb_2(O_2)_4(HtthaO_4)] \cdot 2H_2O$ 4. $(gu)_3[Nb(O_2)_4]$ (1 g, 2.5 mmol) was dissolved in 20 mL distilled water and 5 mL of a 35 wt% H_2O_2 solution. H_6ttha (0.616 g, 1.25 mmol) was added by small fractions while stirring and pH was adjusted down to 3 with nitric acid (1 mol L^{-1}). The resulting clear solution was then gently heated for a few minutes ($T = 60$ °C). The subsequent cooling of the solution with an ice bath following by addition of cold ethanol (150 mL) provided a pale yellow and fine solid. The suspension was stored at 5 °C during 1 h and the precipitate was finally filtered off, washed with ethanol and air-dried (0.94 g, 70%). Found: C, 23.63; H, 4.89; N, 16.91. $C_{21}H_{47}N_{13}Nb_2O_{26}$ requires C, 23.27; H, 4.34; N, 16.81%.

$(gu)_3[Ta_2(O_2)_4(HtthaO_4)] \cdot 3H_2O$ 5. $(gu)_3[Ta(O_2)_4]$ (1 g, 2.04 mmol) was dissolved in 20 mL distilled water and 5 mL of a 35 wt% H_2O_2 solution. H_6ttha (0.506 g, 1.02 mmol) was added by small fractions while stirring and pH was adjusted down to 3 with nitric acid (1 mol L^{-1}). The resulting clear solution was then gently heated for a few minutes ($T = 60$ °C). Its subsequent cooling with an ice bath and addition of cold ethanol (150 mL) yielded a white precipitate. The suspension was stored at 5 °C during a few hours and the solid was then filtered off, washed with ethanol and air-dried (0.73 g, 58%). Found: C, 19.84; H, 3.97; N, 13.79. $C_{21}H_{49}N_{13}Ta_2O_{27}$ requires C, 19.73; H, 3.84; N, 14.25%.

$(gu)_3[NbTa(O_2)_4(HtthaO_4)] \cdot 2H_2O$ 6. $(gu)_3[Nb(O_2)_4]$ (0.82 g, 2.04 mmol) and $(gu)_3[Ta(O_2)_4]$ (1 g, 2.04 mmol) were dissolved in 40 mL distilled water and 10 mL of a 35 wt% H_2O_2 solution. H_6ttha (1.01 g, 2.04 mmol) was added by small fractions while stirring and pH was adjusted down to 3 with nitric acid (1 mol L^{-1}). The resulting clear solution was then gently heated for a few minutes ($T = 60$ °C). The subsequent addition of ethanol (150 mL) and storage at 5 °C during 2 days yielded a white precipitate which was filtered off, washed with ethanol and air-dried (0.76 g, 64%). Found: C, 21.45; H, 4.02; N, 16.16. $C_{21}H_{47}N_{13}NbTaO_{26}$ requires C, 21.51; H, 4.01; N, 15.54%.

$H_5dtpaO_3 \cdot H_2O$ I. H_5dtpa (5 g, 12.7 mmol) was dispersed in 50 mL of glacial acetic acid and 50 mL of a 35 wt% H_2O_2 solution. The suspension was stirred for 24 h at room temperature. The resulting clear solution was then evaporated under reduced pressure (final volume ~10 mL). An equivalent volume of ethanol was added that yielded a white solid which was then filtered off, washed with ethanol and finally air-dried (5.21 g, 89%). Found: C, 36.43; H, 5.60; N, 8.77. $C_{14}H_{25}N_3O_{14}$ requires C, 36.57; H, 5.44; N, 9.14%.

$H_6tthaO_4 \cdot H_2O$ II. This compound was prepared following the same procedure as used for the dtpa derivative I but replacing H_5dtpa with H_6ttha (5 g, 10.1 mmol) (5.02 g, 86%). Found: C, 37.65; H, 6.01; N, 9.16. $C_{18}H_{32}N_4O_{17}$ requires C, 37.50; H, 5.55; N, 9.72%.

2.3. Pyrolysis of the precursors

A sample (approximately 0.5 g) of each ttha complex (**4, 5** and **6**) as well as a ground mixture of **4** and **5** (Nb/Ta molar ratio = 1) were placed in a porcelain dish and pre-calcined at 300 °C for 6 h in air, yielding an amorphous material which was then calcined for 6 h in air, at 700 or 800 °C, depending on the Ta content.

3. Results and discussion

3.1. Complexes

3.1.1. IR spectroscopy

Table 1 lists, for compounds **1–6**, the infrared bands which are assigned to typical stretching vibration modes of the metal M coordinated to side-bonded peroxo ligands ν(O–O), $\nu_{as}[M(O_2)]$ and ν_{as}(O–M–O) as well as some representative vibrational modes of the coordinated carboxylate of the PAC ligand. The infrared spectra also display a band assigned to the stretching of the N–oxide bond, ν(N–O), appearing near 900 cm^{-1} and revealing the in situ oxidation of the nitrogen atoms in the PAC ligand. This phenomenon was previously observed in the case of Nb or Ta complexes with edta and pdta [30,31].

The infrared spectra of the homometallic complexes **1** and **5** display two ν(O–O) bands of medium intensity at 870 and 855 cm^{-1} for the Nb–dtpa derivative and at slighter values, 853 and 841 cm^{-1}, for the Ta–ttha complex. This spectral shape can be assigned to a metal-diperoxo species [30,31,33]. The homometallic compounds **2** and **4** present only one band at 844 and 861 cm^{-1}, respectively, but which is quite broad and probably occurs from two ν(O–O) modes which are very closed to each other. Moreover, the infrared spectrum of the heterometallic complex **6** shows three ν(O–O) bands resulting from the superposition of the bands appearing in the spectra of the corresponding homometallic complexes **4** and **5**, while the spectrum of compound **3** shows only one broad and very weak ν(O–O) band at 857 cm^{-1}.

Next to this, oxidation of the nitrogen atoms of the PAC ligand during the syntheses (excess H_2O_2 medium) is evidenced by the presence, in the infrared spectra of compounds **1–6**, of the ν(N–O) band near 900 cm^{-1}. In the corresponding bis(N-oxide) derivative of the free ligands, $H_5dtpaO_3 \cdot H_2O$ and $H_6tthaO_4 \cdot H_2O$, this band appears at 897 and 900 cm^{-1}, respectively.

3.1.2. Thermal analyses

After dehydration, the dtpa or ttha complexes **1–6** undergo a multi-step degradation into oxides up to a final decomposition temperature in the range 600–750 °C.

The thermograms of the three dtpa compounds **1**, **2** and **3** display a slight weight loss (approximately 3%) corresponding to the last decomposition step, that is characteristic of Nb and Ta compounds. In the case of the homometallic derivatives, this final step appears at 610 °C for the niobium complex **1** and at 740 °C for the tantalum complex **2**. In the thermogram of a 1:1 molar ratio mixture of **1** and **2**, two distinct steps appear at 610 and 740 °C, in line with the presence of the Nb and Ta

Table 1
Infrared data (in cm^{-1}) for compounds **1–6**

		ν_{as}(COO)	ν_s(COO)	ν(N–O)	ν(O–O)	$\nu_{as}[M(O_2)]$	ν_s(O–M–O)
dtpa Ligand	**1**	1658 *sb*	1388 *m*, 1335 *m*	909 *m*	870 *m*, 855 *m*	676 *w*	559 *m*
	2	1653 *sb*	1386 *m*, 1335 *m*	931 *m*	844 *mb*	640 *w*	541 *m*
	3	1663 *sb*	1386 *m*, 1331 *m*	930 *w*	857 *wb*	666 *w*	561 *m*
ttha Ligand	**4**	1651 *sb*	1377 *m*, 1339 *m*	926 *m*	861 *mb*	—*	553 *m*
	5	1655 *sb*	1384 *m*	920 *m*	853 *m*, 841 *m*	—*	538 *m*
	6	1655 *sb*	1383 *m*	912 *w*	860 *m*, 854 *m*, 842 *m*	—*	538 *mb*

*Vibration mode not observed.
Intensity: *s* = strong, *m* = medium, *w* = weak, *b* = broad.

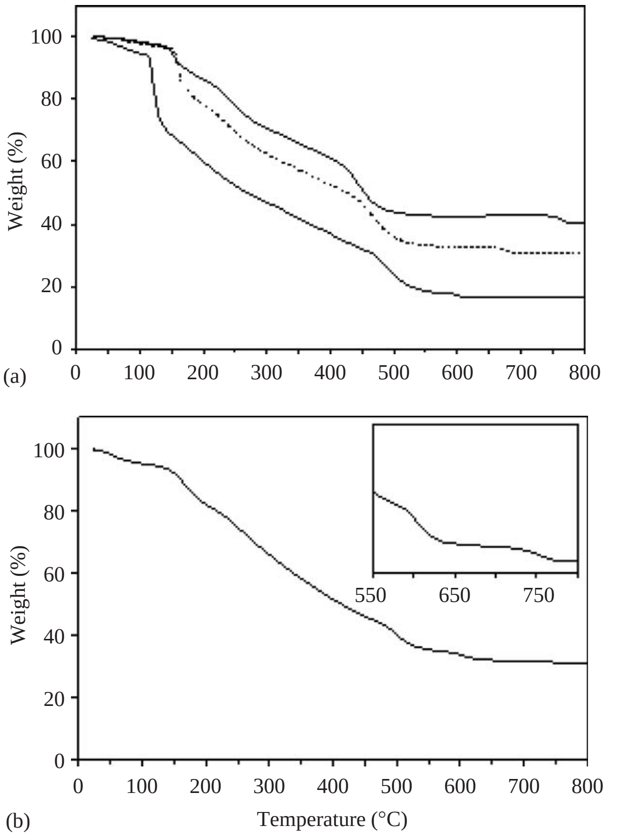

Fig. 1. Thermogravimetric analyses in air of (a) **4** (bold line), **5** (normal line), **6** (straight line), and (b) a 1:1 molar ratio mixture of **4** and **5** (10 °C min^{-1}).

Table 2
Major fragments observed in the mass spectra (anionic mode) of dtpa compounds **1–3**. The experimental m/z values (exp.) are compared to the values calculated (calc.) on the basis of the proposed stoichiometry for the differents anions observed

	Anionic fragments observed		m/z exp.	m/z calc.
1	$(Hgu[Nb_2(O_2)_4(dtpaO_3)])^-$		654.8	655.3
	$(H_2[Nb_2(O_2)_4(dtpaO_3)])^-$		595.8	596.3
	n.i *		375.7	/
	$(gu[Nb_2(O_2)_4(dtpaO_3)])^{2-}$		327.2	327.1
	$(H[Nb_2(O_2)_4(dtpaO_x)])^{2-}$	$x = 3$	297.6	297.7
		$x = 2$	289.3	289.7
		$x = 1$	281.7	281.7
2	$(H[Ta_2(O_2)_4(dtpaO_x)])^{2-}$	$x = 3$	463.7	463.7
		$x = 2$	455.8	455.7
		$x = 1$	447.8	447.7
		$x = 0$	439.8	439.7
3	$(H[Nb_2(O_2)_4(dtpaO_x)])^{2-}$	$x = 3$	298.2	297.7
		$x = 2$	290.6	289.7
		$x = 1$	282.1	281.7
	$\mathbf{(H[NbTa(O_2)_4(dtpaO_x)])^{2-}}$	$\mathbf{x = 3}$	**419.5**	**419.7**
		$\mathbf{x = 2}$	**411.7**	**411.7**
		$\mathbf{x = 1}$	**403.8**	**403.7**
		$\mathbf{x = 0}$	**395.7**	**395.7**
	$(H[Ta_2(O_2)_4(dtpaO_x)])^{2-}$	$x = 3$	463.7	463.7
		$x = 2$	455.6	455.7
		$x = 1$	447.7	447.7
		$x = 0$	439.7	439.7

**n.i* = unidentified fragment.

Table 3
Major fragments observed in the mass spectra (anionic mode) of ttha compounds **4–6**. The experimental m/z values (exp.) are compared to the values calculated (calc.) on the basis of the proposed stoichiometry for the differents anions observed

	Anionic fragments observed		m/z exp.	m/z calc.
4	$(gu[Nb_2(O_2)_4(HtthaO_x)])^{2-}$	$x = 4$	463.2	463.7
		$x = 3$	455.3	455.7
		$x = 2$	447.3	447.7
		$x = 1$	439.4	439.7
		$x = 0$	430.9	431.7
	$(H[Nb_2(O_2)_4(HtthaO_x)])^{2-}$	$x = 4$	433.9	434.2
		$x = 3$	425.9	426.2
		$x = 2$	417.9	418.2
		$x = 1$	409.9	410.2
		$x = 0$	401.9	402.2
5	$(Hgu[Ta_2(O_2)_4(tthaO_4)])^{2-}$		551.2	551.7
	$(H_2[Ta_2(O_2)_4(tthaO_4)])^{2-}$		521.8	522.2
6	$\mathbf{[NbTa(O_2)_4(tthaO_4)]^{4-}}$		**239.3**	**239.1**

homonuclear derivatives, respectively. In the thermogram of compound **3**, one single step occurs at the intermediate temperature of 690 °C, evidencing the heterometallic nature of this compound.

The ttha complexes **4**, **5** and **6** display the same behavior. Their thermograms are illustrated in Fig. 1(a). The last decomposition step appears in the case of the homometallic compounds **4** and **5** at 600 and 750 °C, respectively, while it occurs in the thermogram of complex **6** at an intermediate temperature of 680 °C. Moreover, in the thermogram of a 1:1 molar ratio mixture of **4** and **5**, two distinct steps corresponding to the homometallic species appear at 600 and 750 °C (Fig. 1(b)).

3.1.3. Mass spectrometry

The major anionic fragments observed in the mass spectra of complexes **1–6** are listed in Tables 2 and 3 in the case of the dtpa and ttha derivatives, respectively.

The mass spectrum of compound **1** displays peaks corresponding the parent ion combined either to one H$^+$ and one guanidinium, or to two H$^+$, or to one guanidinium, and which are assignable to the singly charged species $(Hgu[Nb_2(O_2)_4(dtpaO_3)])^-$ and $(H_2[Nb_2(O_2)_4(dtpaO_3)])^-$ and the doubly charged anion $(gu[Nb_2(O_2)_4(dtpaO_3)])^{2-}$, respectively. Moreover, the parent ion combined with one H$^+$, $(gu[Nb_2(O_2)_4(dtpaO_3)])^{2-}$ is also observed along with the ions derived from the successive losses of two oxygen atoms from the N-oxide groups in the $dtpaO_3$ ligand, $(gu[Nb_2(O_2)_4(dtpaO_x)])^{2-}$ ($x = 2$ and 1). This observation provides a further evidence for the in situ oxidation of the nitrogen atoms of the ligand.

The mass spectrum of the corresponding tantalum derivative **2** shows the parent ion combined to one H^+ and its fragments occurring from the successive losses of the three oxygen atoms from the N-oxide groups in the $dtpaO_3$ ligand. This phenomenon leads to the presence of the dianionic series $(H[Ta_2(O_2)_4(dtpaO_x)])^{2-}$ with $x = 3$, 2, 1 and 0.

Next to that, the mass spectrum of the dtpa compound **3** presents several major peaks corresponding to the heteronuclear doubly charged species $(H[NbTa(O_2)_4(dtpaO_x)])^{2-}$ with $x = 3$, 2, 1 and 0. This observation evidences the formation of a mixed Nb–Ta complex. We also observed in that case signals from both corresponding homonuclear derivatives **1** (fragments $(H[Nb_2(O_2)_4(dtpaO_x)])^{2-}$ with $x = 3$, 2 and 1) and **2** (fragments $(H[Ta_2(O_2)_4(dtpaO_x)])^{2-}$ with $x = 3$, 2, 1 and 0). We already evidenced such an observation in heteronuclear Nb–Ta peroxo-tartrato complexes [29]. This was interpreted either by the occurrence of dissociation–recombination phenomena during the spray formation or in gaseous phase, or by the presence of undesirable homometallic species in the analysed solution, which would come from the sample itself or from a dissociation–recombination process in solution that generates the homometallic complexes from the heterometallic one. We also measured the response of a 1:1 molar ratio mixture of both homometallic species **1** and **2** and observed that the mass spectrum obtained evidences the formation of small amounts of the heterometallic complex (peak of relatively low intensity at m/z 419.6) from the two homometallic compounds.

The mass spectrum of the Nb–ttha complex **4**, illustrated in Fig. 2, displays peaks assigned to the parent ion combined either with one H^+, $(H[Nb_2(O_2)_4(HtthaO_4)])^{2-}$, or with one guanidinium counter-ion, $(gu[Nb_2(O_2)_4(HtthaO_4)])^{2-}$. Signals from the successive losses of oxygen atoms from the four N-oxide groups present in the $tthaO_4$ ligand are also present and correspond to the dianionic series: $(H[Nb_2(O_2)_4(HtthaO_x)])^{2-}$ and $(H[Nb_2(O_2)_4(tthaO_x)])^{2-}$, with $x = 4$, 3, 2, 1 and 0.

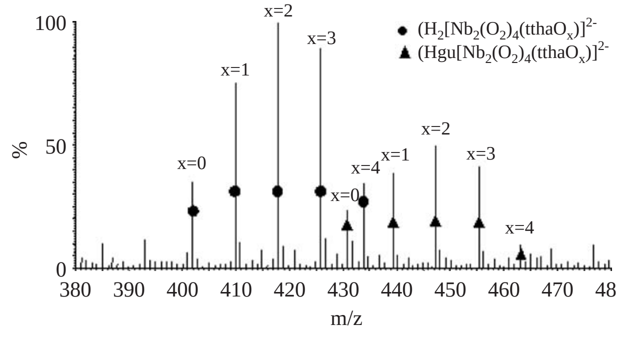

Fig. 2. Nano-electrospray ionization mass spectrum (anionic mode) of compound **4**, $(gu)_3[Nb_2(O_2)_4(HtthaO_4)] \cdot 2H_2O$.

In the case of the Ta compound **5** with ttha, the mass spectrum displays an important background and numerous signals in a low m/z region, probably occurring from the decomposition of the ligand itself. Nevertheless, two peaks of high intensity are detected and assigned to the parent ion combined with one H^+ and one guanidinium, $(Hgu[Ta_2(O_2)_4(tthaO_4)])^{2-}$ or combined with two H^+, $(H_2[Ta_2(O_2)_4(tthaO_4)])^{2-}$.

Finally, we observe, in the mass spectrum of the heteronuclear ttha complex **6**, that most of the peaks are attributed to the decomposition of the ligand $tthaO_4$, as it was first observed in the Ta homonuclear derivative **5**. However, we also detect a signal at m/z 239.3, assigned to the parent ion which has lost one proton, $[NbTa(O_2)_4(tthaO_4)]^{4-}$ (m/z calc. = 239.1). Moreover, it is important to highlight that, contrarily to the dtpa heteronuclear compound **3**, there is no evidence for the presence of the homometallic species.

3.2. *Oxides*

3.2.1. *X-ray diffraction*

The XRD studies of the calcined Nb–Ta samples show that the thermal treatment applied to the precursors leads to crystalline materials for all compositions. Fig. 3 allows comparing the XRD pattern of the oxide obtained from the heterometallic complex **6** with those of the corresponding binary oxides, Nb_2O_5 and Ta_2O_5, obtained from the homometallic compounds **4** and **5**, respectively. The similarity of the diffractograms suggests that the material prepared from **6** is isostructural with orthorhombic Nb_2O_5 (JCPDS file 30-0873) or Ta_2O_5 (JCPDS file 25-0922). However, slight shifts in 2θ

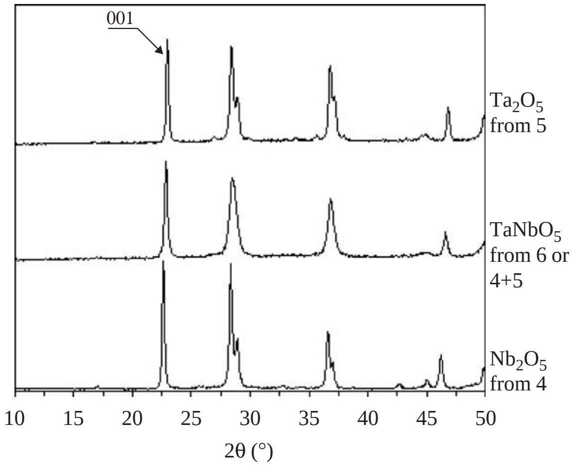

Fig. 3. X-ray diffraction patterns of the $(Ta_xNb_{1-x})_2O_5$ oxides obtained from **4**, **5**, **6** and an equimolar mixture of **4** and **5** ($x = 0$, 1, 0.5).

values are actually observed for several diffraction peaks. The interplanar distance $d(001)$ increases linearly with the tantalum content, x, in the case of the oxides obtained from the ttha precursors **4**, **5** and **6** as well as the equimolar mixture of **4** and **5**. A similar trend of the lattice evolution has been previously observed [13,15,34] but cannot be rationalized on the basis of the respective ionic radii of Nb^{5+} and Ta^{5+}, which are identical (0.74 Å) [35]. This behavior evidences the formation of the ternary oxide $TaNbO_5$, corresponding to the $(Ta_xNb_{1-x})_2O_5$ solid solution with $x = 0.5$, by calcining the heterometallic complex **6**. Next to that, the pyrolysis of a 1:1 molar ratio mixture of **4** and **5** gives the same XRD results as for **6**.

3.2.2. *Raman spectroscopy*

The Raman analyses of the Nb–Ta oxides prepared confirm the formation of a $TaNbO_5$ solid solution from the thermal treatment of **6** because (i) the Raman spectra observed in both cases are similar to those obtained from **4** or **5** and (ii) we observe a linear variation of the position of several Raman bands with the composition. When the Ta content increases, these bands are shifted to lower wavenumbers, in line with the fact that Ta is heavier than Nb. A similar behavior was previously observed for the $(Ta_xNb_{1-x})_2O_5$ solid solution [34].

3.2.3. *BET and SEM*

BET and SEM measurements have been carried out to study the morphology of the oxides produced from the thermal decomposition of the prepared complexes.

While the specific surface areas of the oxides obtained from **4**, **5**, and the 1:1 mixture of **4** and **5** are 1.3, 14, and 12 $m^2 g^{-1}$, respectively, the material obtained from **6** displays a larger value of 19 $m^2 g^{-1}$. These results indicate that the use of the heterometallic precursor **6**

Table 4
Specific surface areas (BET method) of the Nb–Ta oxides prepared from the ttha precursors

Precursor	S_{BET} ($m^2 g^{-1}$)
4	1.3*
5	14
6	19
Equimolar mixture of **4** and **5**	12

*Measurement carried out by krypton adsorption.

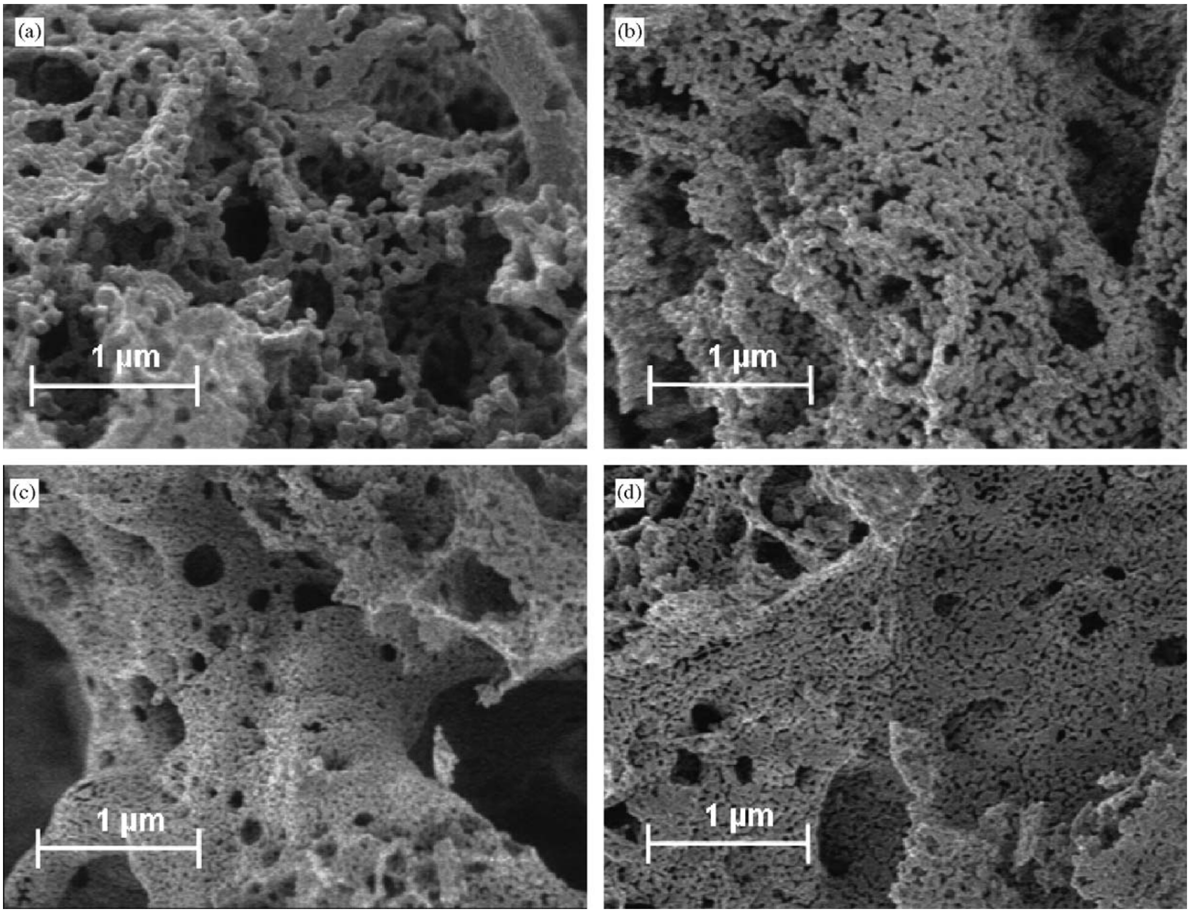

Fig. 4. SEM images of the oxides obtained from (a) **4**, (b) **5**, (c) **6**, and (d) a 1:1 molar ratio mixture of **4** and **5**.

allows the preparation of mixed oxides with higher specific surface area. This phenomenon was already observed for oxides obtained from a Nb–Ta heterobimetallic peroxo-tartrato complex [29] (Table 4).

SEM images of the oxides obtained are illustrated in Fig. 4. The mixed $TaNbO_5$ phase prepared from **6** or from the mixture of **4** and **5** displays a porous character, mainly revealing mesopores but also some macropores (Figs. 4(c) and (d), respectively). No significant morphology difference is observed between both pictures except that the pores are slightly smaller in the first case, in line with the fact that this oxide possesses a higher specific surface area. Moreover, the SEM images of the binary phases Nb_2O_5 and Ta_2O_5 obtained from the homonuclear compounds **4** and **5**, respectively, reveal they practically display a non-porous character, especially in the case of Nb_2O_5.

4. Conclusion

New homo- and heterobimetallic peroxo niobium^{V} and tantalum^{V} complexes with high-denticity polyaminocarboxylato ligands have been prepared and characterized. The thermal decomposition in air of the complexes was shown to provide binary (Nb_2O_5 or Ta_2O_5) or ternary ($TaNbO_5$) oxides with interesting morphology and surface characteristics. The use of a heterometallic Nb–Ta complex as a "single-source precursor" presents several advantages from the point of view of preparation and material properties. Because these complexes are quite easily prepared, are stable toward moisture and highly soluble in water, they constitute ideal candidates as molecular precursors for Nb and/or Ta-based materials (bulk or supported oxides, films and coatings).

Acknowledgments

The authors thank the Belgian National Fund for Scientific Research (FNRS) for the research fellowship allotted to D.B. and financial support. They also thank *CBMM Company* (Brazil) and Niobium Products Company GmbH (Germany) for supplying niobic acid and their financial support, and Prof. R. Legras for access to the SEM equipment.

References

[1] P. Ayyub, M.S. Multani, V.R. Palmkar, R. Vijayaraghavan, Phys. Rev. B 34 (1986) 8137.
[2] T. Okubo, M. Kakihana, J. Alloy Compd. 256 (1997) 151.
[3] T. Katou, D.L. Lu, J.N. Kondo, K. Domen, J. Mater. Chem. 12 (2002) 1480.
[4] T. Katou, B. Lee, D.L. Lu, J.N. Kondo, M. Hara, K. Domen, Angew. Chem. Int. Ed. 42 (2003) 2382.
[5] J.N. Kondo, T. Yamashita, T. Katou, B. Lee, D. Lu, M. Hara, K. Domen, Stud. Surf. Sci. Catal. 141 (2002) 265.
[6] Z.G. Zou, J.H. Ye, H. Arakawa, Solid State Commun. 119 (2001) 471.
[7] Z.G. Zou, J.H. Ye, H. Arakawa, J. Mater. Res. 16 (2001) 35.
[8] Z.G. Zou, J.H. Ye, H. Arakawa, Chem. Phys. Lett. 333 (2001) 57.
[9] T. Ushikubo, Catal. Today 57 (2000) 331.
[10] T.C. Watling, G. Deo, K. Seshan, I.E. Wachs, J.A. Lercher, Catal. Today 28 (1996) 139.
[11] Z.G. Zou, H. Arakawa, J.H. Ye, J. Mater. Res. 17 (2002) 1446.
[12] J.M. Amarilla, B. Casal, E. Ruiz-Hitzky, J. Mater. Chem. 6 (1996) 1005.
[13] O. Yamagushi, D. Tomihisa, M. Shirai, K. Shimizu, J. Am. Ceram. Soc. 71 (1988) 260.
[14] M. Zafrir, A. Aladjem, R. Zilber, J. Solid State Chem. 18 (1976) 377.
[15] B. Lee, T. Yamashita, D.L. Lu, J.N. Kondo, K. Domen, Chem. Mater. 14 (2002) 867.
[16] E.R. Camargo, M. Kakihana, Solid State Ion. 151 (2002) 413.
[17] H. Wullens, D. Leroy, M. Devillers, Int. J. Inorg. Mater. 3 (2001) 309.
[18] S. Boulmaaz, R. Papiernik, L.G. Hubert-Pfalzgraf, B. Septe, J. Vaissermann, J. Mater. Chem. 7 (1997) 2053.
[19] L.G. Hubert-Pfalzgraf, Inorg. Chem. Commun. 6 (2003) 102.
[20] J.H. Thurston, K.H. Whitmire, Inorg. Chem. 41 (2002) 4194.
[21] J.H. Thurston, K.H. Whitmire, Inorg. Chem. 42 (2003) 2014.
[22] P.A. Shcheglov, D.V. Drobot, G.A. Seisenbaeva, S. Gohil, V.G. Kessler, Chem. Mater. 14 (2002) 2378.
[23] A.C. Jones, H.O. Davies, T.J. Leedham, P.J. Wright, M.J. Crosbie, A. Steiner, J.F. Bickley, P. O'Brien, A.J.P. White, D.J. Williams, J. Mater. Chem. 11 (2001) 544.
[24] A. Johansson, M. Roman, V.G. Kessler, J. Sol-Gel Sci. Technol. 19 (2000) 725.
[25] L.G. Hubert-Pfalzgraf, Polyhedron 13 (1994) 1181.
[26] P. Werndrup, V.G. Kessler, J. Chem. Soc. Dalton Trans. 5 (2001) 574.
[27] L.G. Hubert-Pfalzgraf, J.G. Riess, Inorg. Chem. 14 (1975) 2854.
[28] M.K. Sharma, A. Singh, R.C. Mehrotra, Trans. Met. Chem. 27 (2002) 115.
[29] D. Bayot, B. Tinant, M. Devillers, Inorg. Chem. 44 (2004) 1554.
[30] D. Bayot, B. Tinant, B. Mathieu, J.P. Declercq, M. Devillers, Eur. J. Inorg. Chem. (2003) 737.
[31] D. Bayot, B. Tinant, M. Devillers, Inorg. Chem. 43 (2004) 5999.
[32] B. Beltran Porter, M. de Haro Rodriguez, P. Penalver Conesa, Afinidad 33 (1976) 489.
[33] D. Bayot, B. Tinant, M. Devillers, Catal. Today 78 (2003) 439.
[34] D. Bayot, M. Devillers, Chem. Mater. 16 (2004) 5401.
[35] R.D. Shannon, Acta Crystallogr. A 32 (1976) 751.